Using a Semi-Staging approach to Improve Oil Scoop Capture Efficiency

Akinola A. Adeniyi *[α] and Kirijen Vengadasalam[β,α]

[α] School of Engineering and Computing, University of Central Lancashire, PR1 2HE, United Kingdom.

[α]https://orcid.org/0000-0003-0768-9341, [β] https://orcid.org/0009-0001-3308-6619

Abstract

Spatial and weight restrictions on very high performance aeroengines require more advanced and efficient lubrication systems. An oil scoop is a device that aims to capture a jet of oil to feed high-speed bearings by directing the oil jet along the axial direction of the shaft via under-race feed to the bearing elements. Splashing is a prominent oil-morphology feature in oil scoop dynamics. Splashing happens after the oil jet impacts on the rotating oil scoop blades resulting in a centrifugally outward loss of oil. These loses contribute oil capture inefficiencies. There are optimisation approaches with the aim of limiting blades' leading and trailing edge interaction with the oil jet in open literature. There are none, however, that has attempted to recapture the centrifugal losses to form part of the bearing feed, potentially needed to improve the overall oil capture efficiency. This, however, creates an additional challenge of driving the lubricants against centrifugal and gravitational forces towards a set of "bearing scoops" in stage 3. In this work, we attempted to capture the lubricants against these forces with vanes and results show a chance to achieve lubrication almost before the first shaft revolution. 2D CFD simulation shows a very good potential with this staging approach to improve scoop overall capture efficiency.

Keywords: Oil scoop; Staged-scoop; Under-race lubrication.

1 Introduction

Oil lubrication is preferred over grease in aeroengines because it provides better cooling and continuous lubrication under high-speed and high-load conditions, essential for preventing overheating and ensuring components longevity (Glahn and Wittig 1996; Dai et al. 2022). To "get" the oil into the bearings is, however, challenging because of the ensuing splashing that will result from the contact of a jet of oil with a solid rotating component (Paleo Cageao et al. 2019; Jiang et al. 2023) and also from the nature of flow physics of oil and air (Adeniyi et al. 2017). Splashing (including atomisation into droplets) is not desirable in an engine because it represents inefficiency in capturing the lubricant into the bearing (Paleo Cageao et al. 2019) and pose further challenge to separate from the oil-air mixture (Eastwick et al. 2006; Zhang et al. 2020). The operating environment of the bearing is very hot (Zhong et al. 2023), therefore splashing of oil droplets should be minimised as much as possible to avoid potential smoke from hot surface ignition (Willenborg et al. 2002).

Aeroengine bearings are susceptible to failure due to factors like improper lubrication and material stress under extreme high-speed and high-load conditions (Kumar and Satapathy 2023). They must meet stringent requirements, including high reliability, smooth operation, low friction, dimensional stability under pressure, minimal vibrations and noise, high-temperature resistance, the ability to function briefly "without lubrication", easy maintenance, specified lifespan, and reduced weight (Kumar and Satapathy 2023). These challenges necessitate advanced design and precise engineering to ensure optimal performance and durability.

*✉ aadeniyi@uclan.ac.uk

Underrace lubrication is a technique used to lubricate aeroengine-bearings by delivering oil (lubricant) directly to its interstitial spaces and rolling elements directly via the under-race. Oil is supplied into the bearing cavity through apertures in the inner-race, utilising centrifugal force and high pressure to ensure optimal lubrication and cooling within roller bearings (Gao et al. 2019). This method is to ensure an adequate film of lubricant, which reduces friction, wear, and heat generation gets to the rolling elements and contact points.

2   STAGED SCOOP CONCEPT

Existing underrace lubrication system concepts (Lee et al. 2020; Jiang et al. 2021; Jingwen et al. 2021), typically, implemented through a jet of oil aimed at a rotating set of blades (oil scoops) that capture the oil along a radial direction of the shaft and direct the flow axially into the bearing elements as shown schematically in Fig. 1. The captured oil is directed into the underrace feed channel before it becomes "used oil". The used oil is then captured inside an air pressurised bearing chamber (Adeniyi et al. 2015; Ren et al. 2023).
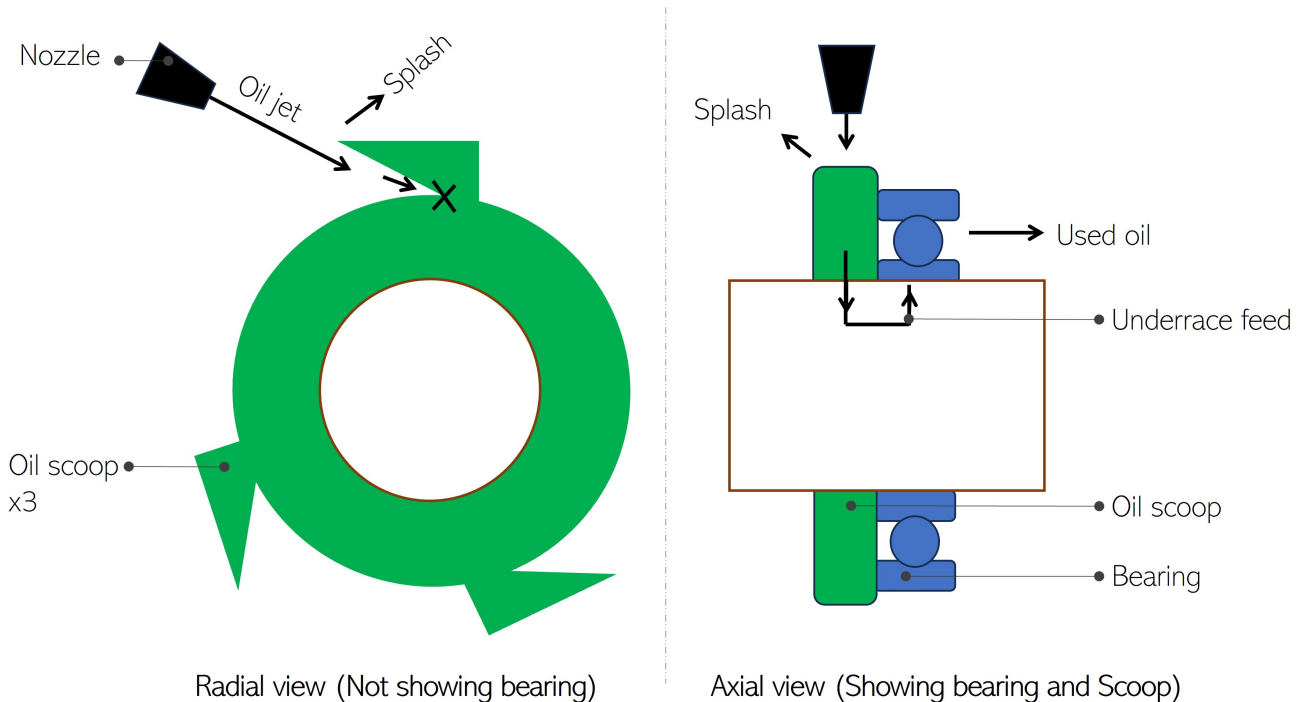
Figure 1: A schematic of existing scoop design

The used oil is then pumped and filtered before re-use. The amount of oil splashed is significant depending on the design of the scoop. The capture efficiency of oil scoop is known to be dependent on factors such as shaft speed, the jet angle, the oil jet flow speed (Paleo Cageao et al. 2019; Jiang et al. 2023). The reported range of efficiencies in the open literature for related oil scoops range from 19% to 81% depending on different configurations. It can be noted that the direction of the splash is centrifugally outwards from the shaft/scoop. This is the direction of the losses from splash resulting from the impact of the oil jet on the rotating scoops.

Our idea, as in Fig. 2 is, therefore, to capture flow in "semi-stages", whereas in the first stage, the "inverted scoops" receive the jet of oil. It is expected that there will still be splashing in stage 1 at the jet-scoop impact but the resulting splash is expected

(in theory) to also be captured within that volume by the other inverted scoops. We expect no or minimal radially outward losses in stage 1 or in other words, the efficiency in stage 1 is expected to be near 100%. In this paper, the scoops in stage 1 are referred to as "inverted-scoops".
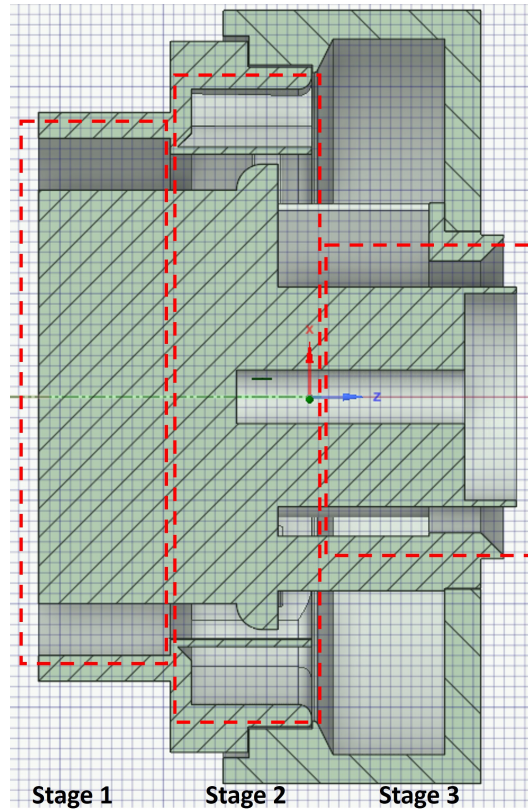
(a) Cross-section along the shaft
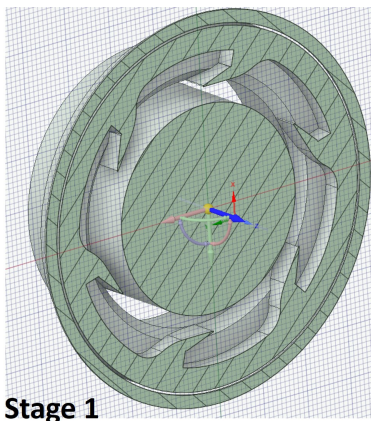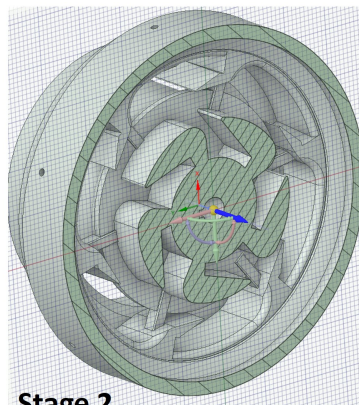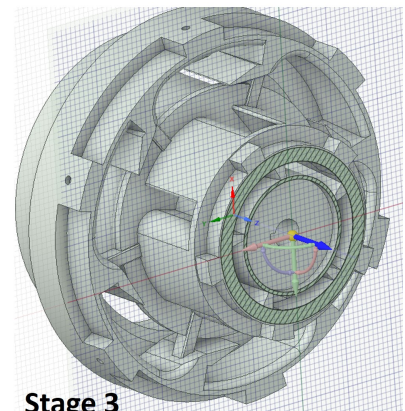
(b) Isometric Sectional Views

Figure 2: A section view through the staged-scoop design - CAD

The oil captured in stage 1, by a proper design of the inverted blades, then directs the into a buffer stage 2. In stage 3, the flow enters into the rotating scoops that feeds into the underrace channel. In this paper, the scoops in stage 3 that feed into the underrace channel are referred to as "bearing-scoops".

55

This solution also creates a new challenge for the captured oil in stage 2 to get into the bearing-scoops. The oil in stage 2 is still having high outward radial momentum significantly against gravity ($m\omega^2 R / m \cdot g >> 1$). Even if this ratio is close to unity or lower, pooling of the oil at the bottom of the cylinder (stage 2) is expected. Pooling in stage 2 would result in axially outward loss of lubricant. The staging challenge is therefore the ability to redirect a filling flow from a larger cylinder into a smaller cylinder against both gravity and centrifugal force. This is, however, not the same problem as an liquid impeller flow (or reverse impeller/turbine). In the case of an impeller/turbine, the control volume is closed but in this multiphase flow problem, stage 1 is open to air and a jet of oil.

3   EXPERIMENT: OIL SCOOP TEST RIG

A simple visualisation test rig has been developed to study the conceptual oil scoops as shown in Fig. 3. The scoops are made using 3D printed technique with PLA. The bearing-scoop diameter is $100mm$ and the stage 2 diameter can reach $200mm$. The test rig is made of perspex for easy see-through using a high-speed camera (Photron Mini UX100) and operates under atmospheric conditions. Water is used in our experiments, at room temperature, in place of "engine oil" for easy handling and similar to published works (Chandra et al. 2010; Simmons and Chandra 2014) considered "close" to the engine oil at aircraft operating conditions (ExxonMobil n.d.).

(a) CAD Model   (b) Test rig (a side view)
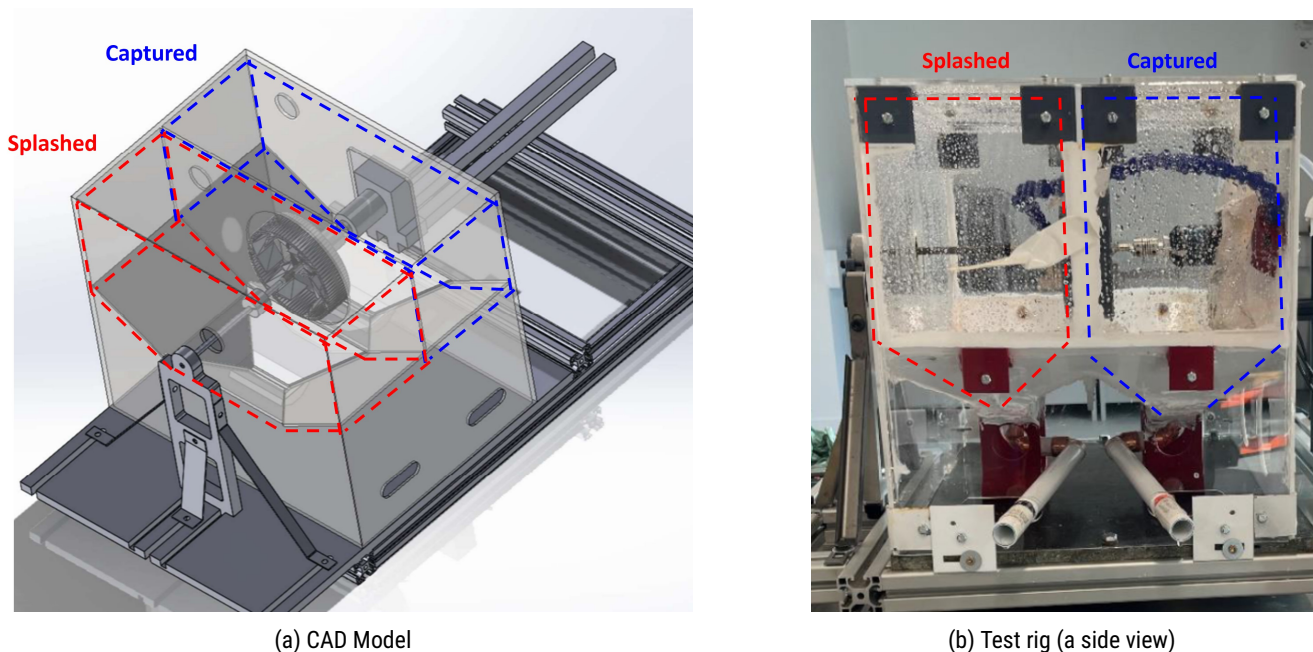
Figure 3: A view of the test rig

There are 2 chambers as shown. The splashed liquid, from the jet impact on the inverted-scoops, are captured into the "splashed" chamber and while the "Captured" chamber collects the volume representing the flow into the bearing. Although with this test rig, it is easy to visualise the external flows around stages 1 and the exit of stage 3, it is prone to some amount of error resulting from the retained amount of liquid on the perspex owing to surface tension Fig. 3b.

It is possible to test a range of configurations in the rig. A closer look into the rig, Fig. 4 shows how the jet is aimed at different angles (Fig. 4a:the jet is aimed at 7'O clock blade from 3 O'clock, whilst the scoop is rotating clockwise).

(a) Front view of the rig

(b) Side view of the rig
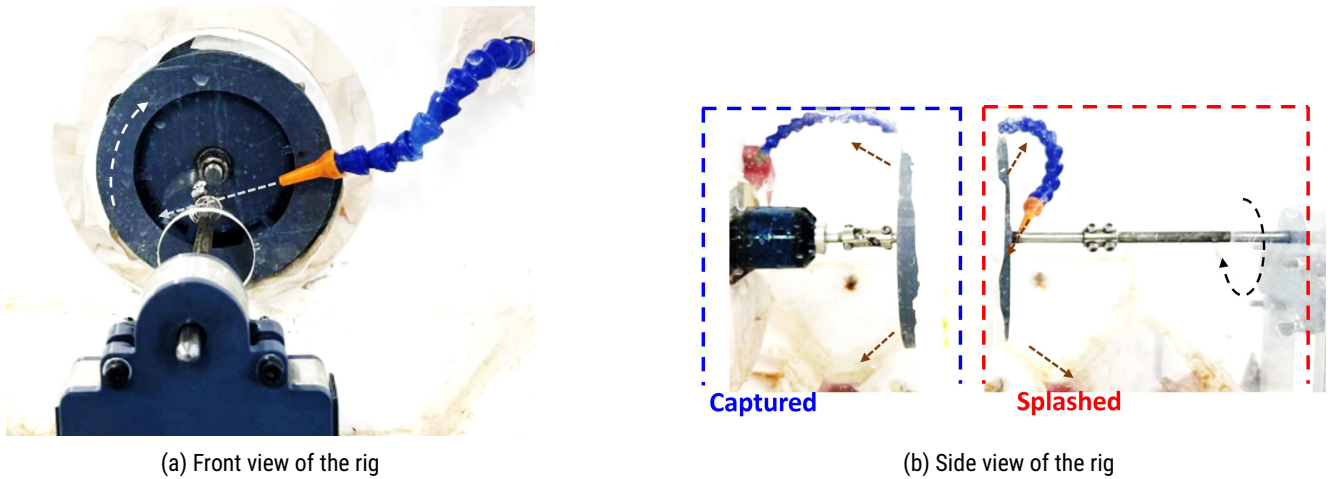
Figure 4: Test rig showing the scoop, jet, captured and splashed zones

(a) Signs of failing blade

(b) Failed blade
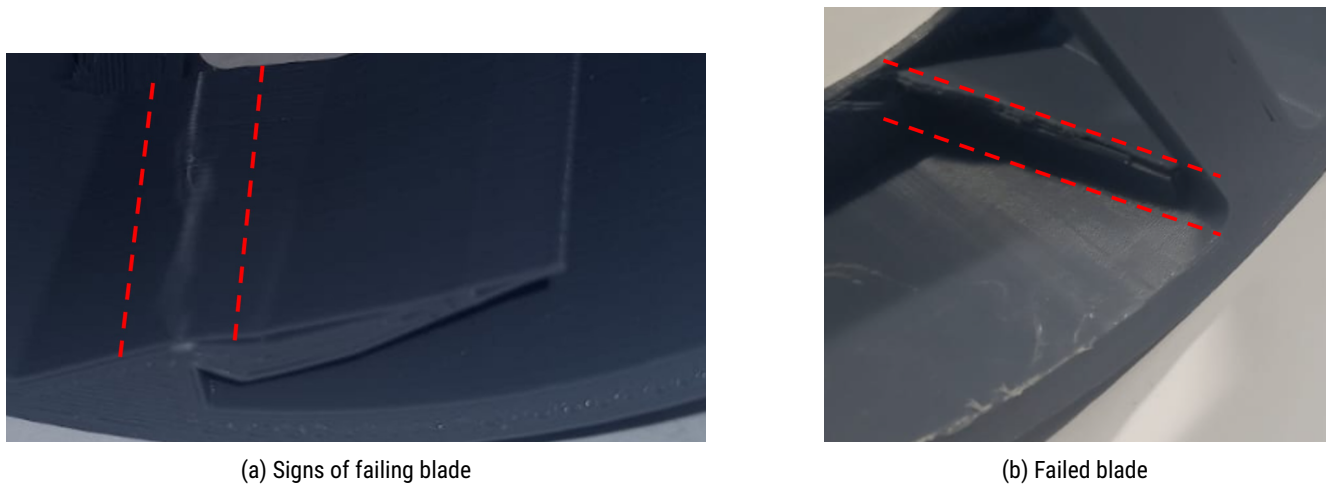
Figure 5: Scoop blade failures from stress

3.1   Experiment: Additive Manufacturing of Scoops

We have used 3D printing (Additive Manufacturing) technique to manufacture the different conceptual scoop designs using PLA (Polylactic Acid) materials. PLA has good ultimate tensile strength (UTS) of about 20.3MPa which can also be increased by blending with other 3D printing materials such as ABS (Dhinesh et al. 2021), To ensure good radial stress distribution and balance, the printing was done using radial filling method. The motor, from a quadcopter, can theoretically reach speeds up to 15,000RPM depending on the applied voltage.

The nozzle diameter range from 0.4mm to as large as 3.5mm and the pump delivering water up to 4 litres/minute. The combination of the radial stress on the PLA-based scoop and impacting jet velocity can cause damage the scoop blades as shown in Fig. 5. This was not common during the experiments but it was observed in one set of our experiments. After several cycles of loading, some of the scoop/blades showed initiation of failure (Fig. 5a) and complete failure (Fig. 5b) on the same scoop. It is therefore important to design the blades for strength and use a fine quality print for the blades.

The 3D printing approach offers a lot of flexibility to test different concepts but a fused/complete printing becomes challenging because of the need for the use of 3D printing supports structures within the volume during printing. The parts

(a) Before coupling

(b) After coupling
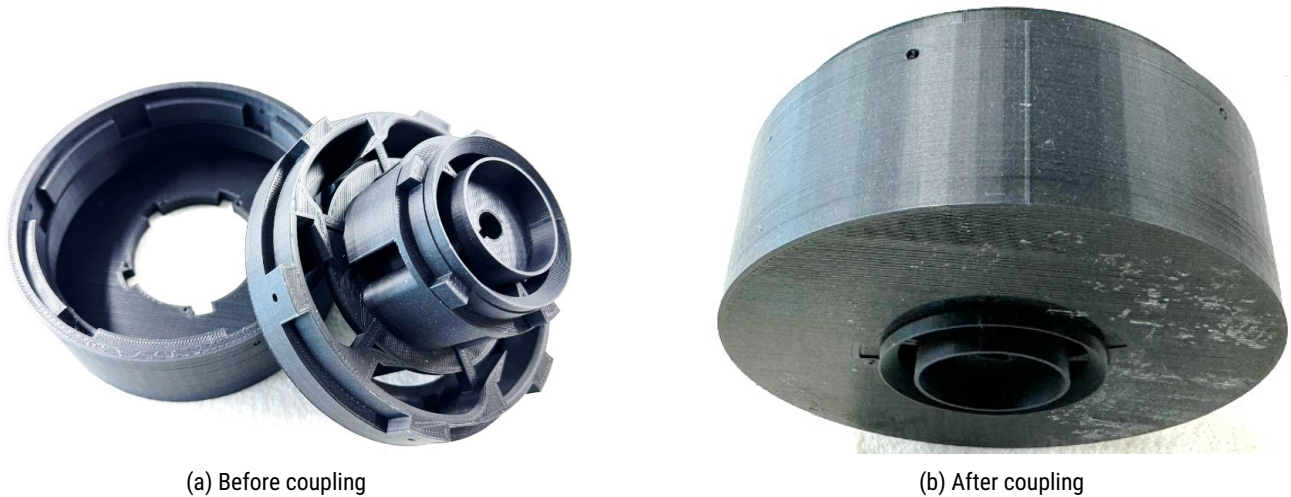
Figure 6: 3D Printed Model

are therefore printed in parts and then coupled. Like this, the "stages" are printed separately (Fig. 6a) and then coupled after (Fig. 6b).

4   NUMERICAL/CFD MODEL: Oil Scoop Test Rig

This paper looks into the flow problem of stage 3 (Fig. 2a) of the stage-scoop, with the goal to be able to get the flow into the bearing-scoop. Finite volume computation fluid dynamics (CFD) approached has been used. The flow is obviously 3 dimensional everywhere in the scoop but we have taken a 2 dimensional approach to observe the possibility to "down come" flow against gravity and centrifugal force. The flow is similar to a rimming flow (Lopes et al. 2018; Sadeghi et al. 2022), i.e., a flow type where there is a fluid inside a partially filled cylinder that is spinning along a horizontal axis, but unlike it, the fluid is, additionally, continually filling up on the circular walls (i.e., from stage 2) and then drained off towards the centre of the cylinder against centrifugal and gravitational forces. In this work, it is to get the flow from an external diameter of 128mm to a diameter of 50mm through outlets of 5mm width. These dimensions are based on our test rig space restrictions/dimension. To model this feed into the rotating cylinder, an inlet velocity boundary is set. There are pressure outlets (named Out1, Out2, ...) depending on the number of outlets. These outlets are placed under the forward faces of the scoop blades representing the capture of the lubricant into the bearings, see Fig. 7.

The flow is turbulent and highly rotational. The $\kappa - \omega$ SST Reynolds Averaged Navier-Stokes (RANS) model has been applied. The flow is a multiphase flow of air and water. The two phases are modelled using the Volume of Fluid (VoF) method. The fluids are solved as a "single fluid" but individually identified with "colour function" (α) advected as in Eq. (1c). In the VoF method, the phases, α, ranges within $0 \leq \alpha \leq 1$ and a clear interface often defined with an iso-surface where $\alpha = 0.5$. Defining one of the phases as the primary, in this case for example, $\alpha \leq 0.5$ would represent air and $\alpha > 0.5$ represents water, e.g. $\alpha = 1$ means purely water is present in the cell volume. The single fluid approach then means only one momentum (Navier-Stokes) equation, Eq. (4), and continuity equation (of the form Eq. 3) are solved, rather than solving these equations for both phases. The conservation is constrained with Eq. 1a; where α_a and α_w are, respectively, the volume fractions of air
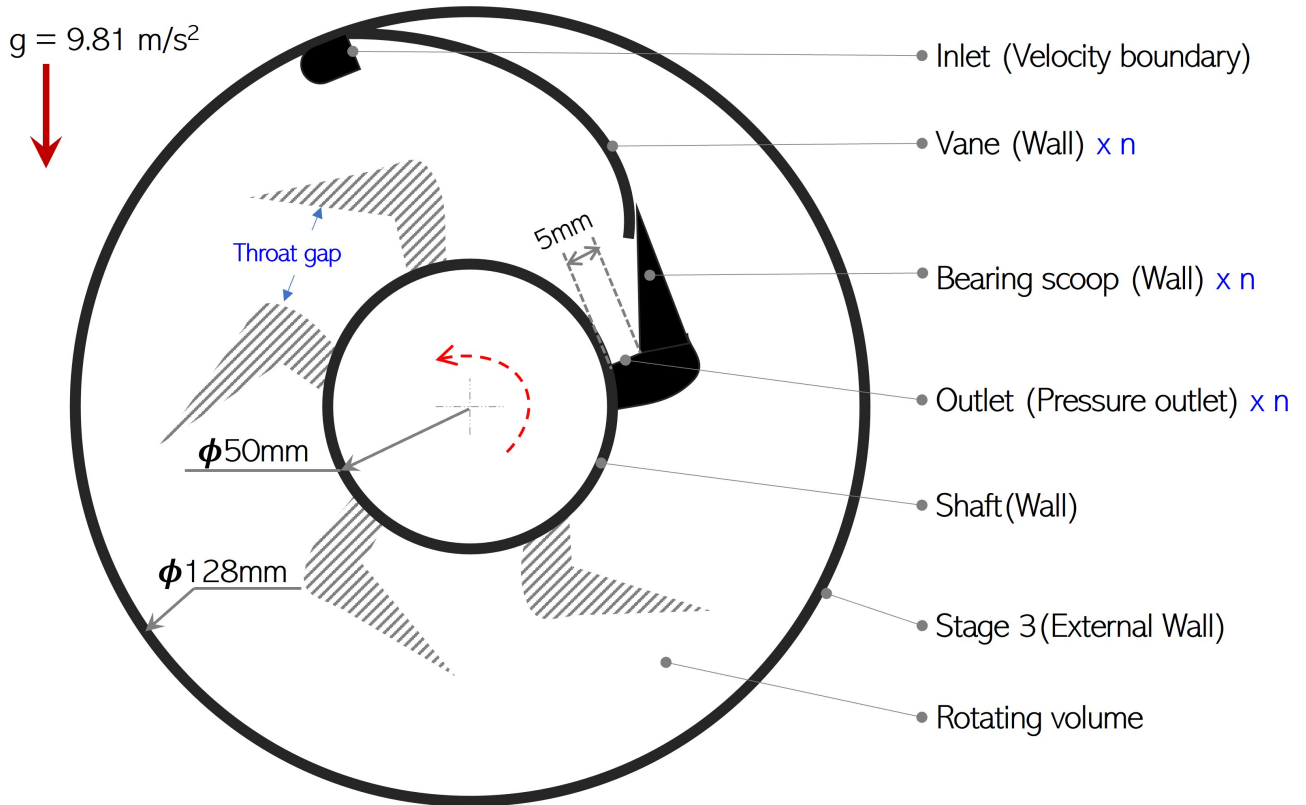
Figure 7: Geometry and Boundary Conditions (showing only one scoop blade/vane)

and water. Fluid properties Φ, e.g., (density (Eq. 2b) and viscosity (Eq. 2c)) are averaged out from the volume fractions from the reference values (Eq. 2a).

$$1 = \alpha_a + \alpha_w \tag{1a}$$

$$\alpha = 1 - \alpha_a \tag{1b}$$

$$\frac{\partial \alpha}{\partial t} + u \cdot \nabla \alpha = 0 \tag{1c}$$

$$\Phi = \sum_{i=1}^{n} \Phi_i \alpha_i \tag{2a}$$

$$\rho = \rho_w \alpha_w + \rho_a \alpha_a \tag{2b}$$

$$\mu = \mu_w \alpha_w + \mu_a \alpha_a \tag{2c}$$

$$\frac{1}{\rho_i} \left[\frac{\partial (\alpha_i \rho_i)}{\partial t} + \nabla \cdot \left(\alpha_i \rho_i \vec{u} \right) = 0 \right] \tag{3}$$

$$\rho\left(\frac{\partial \overrightarrow{u}}{\partial t} + \overrightarrow{u} \cdot \nabla\left(\overrightarrow{u}\right)\right) = -\nabla P + \rho \overrightarrow{g} + \nabla \cdot \mu\left[\nabla \overrightarrow{u} + \left(\nabla \overrightarrow{u}\right)^{T}\right] \tag{4}$$

The transient simulations have been run at $1\mu s$ timestep to ensure the Courant Fredrick Lewy (CFL) number is maintained below 1.0 to be stable. The flow simulated are from 1,000 to 15,000 RPM. The 2D mesh meshes are quad dominant and refined
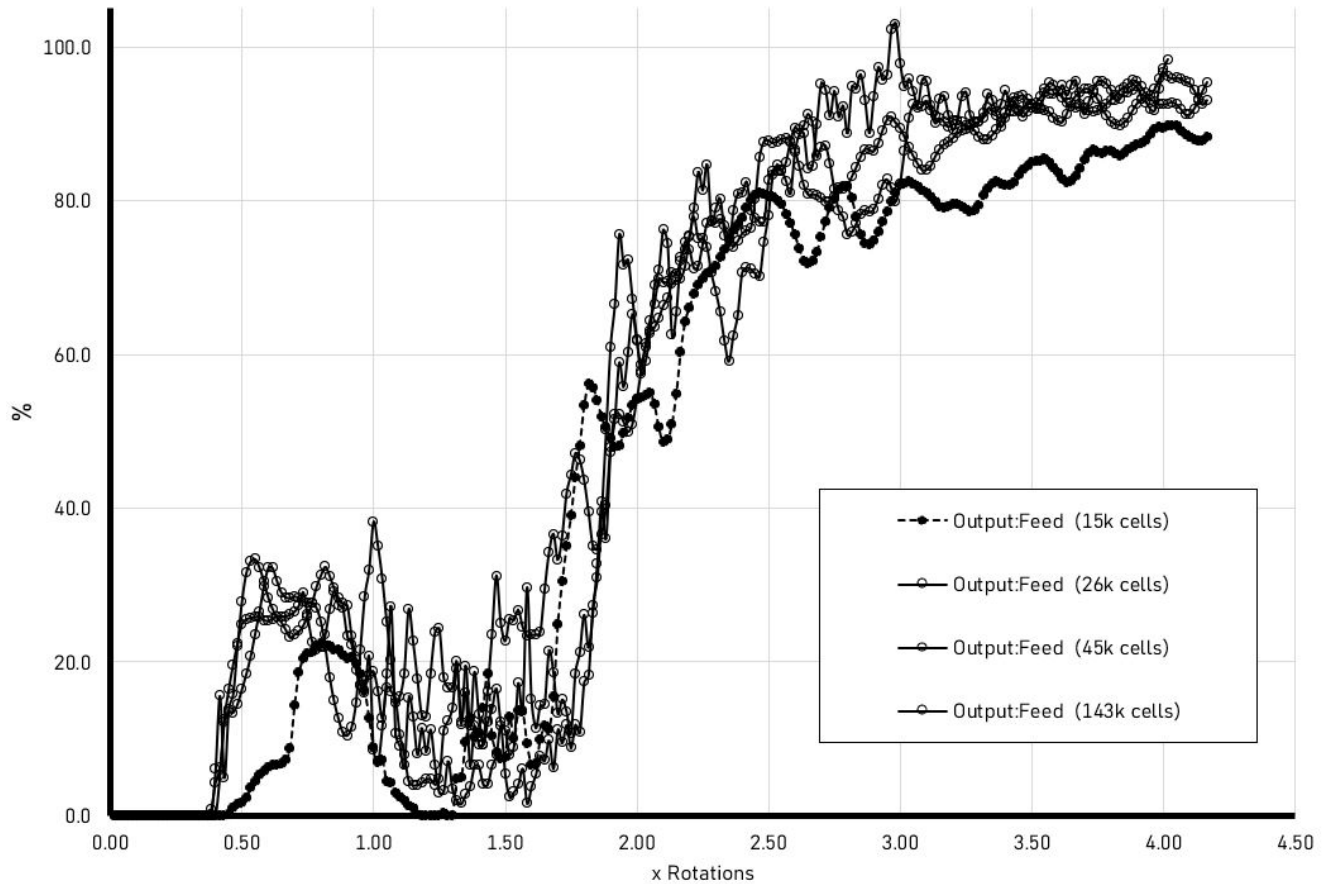
Figure 8: Mesh independence test (5,000 RPM)

everywhere.

4.1 Mesh Independence Test

The mesh density varied from 15,000 to 143,000 cells in the mesh independence tests at 5,000 RPM. Figure 8 shows the mesh independence test done on the 5-vane scoops (Fig. 12), by computing the total outflow from the Outlets into the bearing (i.e., lubrication) measured as a ratio (percent) of the outlet flow to the inlet flow on the vertical against the number of rotations made by the scoop so far. This shows that mesh density of 26,000 cells was reasonably sufficient for this 2D exercise. The flow data is saved every $100\mu s$ for data processing.

5 RESULTS

5.1 Experiment Observations

Figure 9 shows two different experiments. In A1 to A4, the jet is aimed on the bearing scoop (see schematic in Fig. 1). This 125 figure shows the loses from the centrifugal effect creating a continuous splashing on the nozzle face at frequency depending on the number of blades. The arrangement of the images is in an increasing order of flow time, with position A3 showing an instance of the splashing onto the nozzle. The splashing on the nozzle shows that there is continuous loss from the scoop blades as it goes around and still manages to get around to splash onto the face of the nozzle (the original source). The nature of splash comprise of tiny droplets and ligaments of splashes. Whereas B1 to B4 (Fig. 9) shows the jet interaction with the 130 inverted scoops of stage 1 (see the blades in Fig. 2b). This shows that even a larger feed rate of jet, there is lesser splashing (loss) in the inverted scoop but there is still atomisation noticed. The main quantity of flow is inwards into the stage 2 as expected however windage still manages to push the tiny droplets outwards.
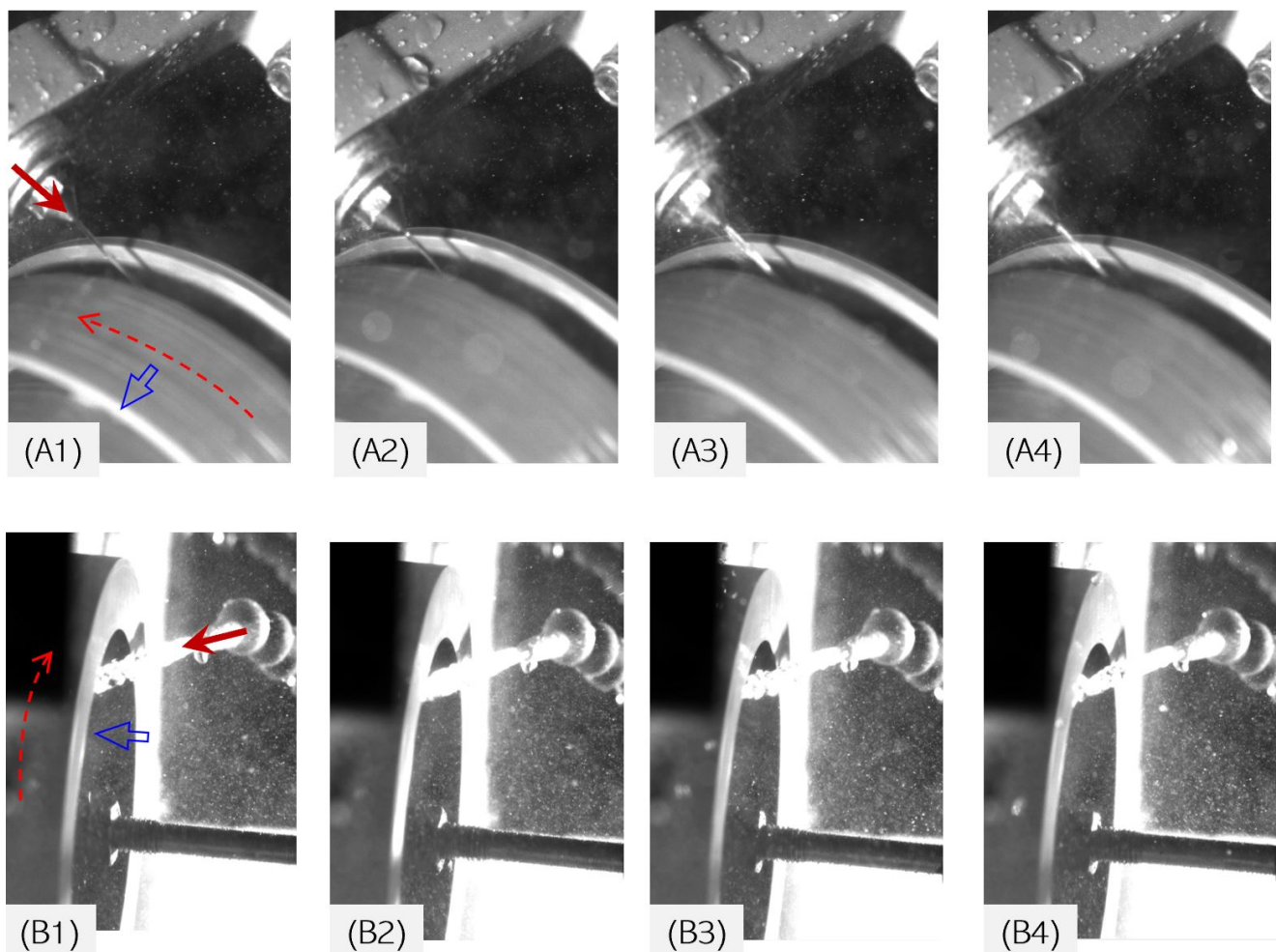
Figure 9: Experimental view of the scoop

5.2   CFD Observations

Figure 10 shows the behaviour of stage 2 for different configurations, all spinning counter clockwise. Each column represent different configuration and the time evolution is from top of the image to the bottom. In, Fig. 10 (A), there are no vanes directing the flow into the bearing scoops. The idea here is that that stage 1 eventually creates a rain of flow for the bearing scoop to capture. The animation shows the flow creates a growing "rimming flow" before eventually touching the tips of the bearing scoops to capture. The stage is then filled up as the time progresses. It takes several rotations before there is any chance of lubrication with this geometry. It should be noted however that in the real problem, the rotating volume is not fully sealed and thus, the "filling rimming" flow would actually exit back into the inlet jet area as splash from stage 1. Thus this is not a good design.

In (B), a set of curved vanes (similar to an impeller) were used. The initial stages shows a promise that the flow goes directly into the bearing scoop region but after a few rotations, the bearing gets no lubricants. Rather, the flow reverses with vortexes on the vanes and then then start to create a growing riming flow similar to (A). This also offers no much difference than geometry (A).

The idea in (D), or the 90° vanes is to create a "shock" to the growing riming flow that will direct the flow into the bearing scoops. This is similar in concept with the 45° vanes (C) but with less shock or stall. These both also create vortexes/stall and lots of recirculation in geometry.

The concept in (E) is to have a set of "drops" from the outer diameter before enntering the bearing scoop. This also generated lots of recirculation and do not necessarily result in instantaneous lubrication. After a long time, and because of continuity, the volumes in all cases end up being filled.

A quantitative measure for the flow output to feed ratio (from one outlet) is shown in Fig. 11a against the number of rotations for 45° and 90° vanes at 10,000RPM. This shows that it takes 6 rotations and just over 7 rotations, respectively, for these scoops before any chance of lubrication is obtained. In both cases, the volumes immediately fill up the volume after the initiation of lubrication. The 90° vane shows a drop resulting from stall and backflow after the 9th rotation. An efficient capture in stage 1 would mask the inefficiency of stage 3, i.e., it is simply accumulating water for the first 6 to 7 rotations without resulting in "lubrication". This also suggests that a backflow into stage 1 would be prominent immediately after filling past an initial volume (in stage 2) and then resulting in a high overall inefficiency of the staged-scoop.

Figure 12 is the result of the CFD simulation of staged-vane scoop (i.e., stage 3). In this staged-vane concept, note that the vanes are not fused to the bearing scoops (because of the need to install as different components). The vanes are smooth (in between the 45° and the 90° types).

The black curve is the data for shaft speed at 1,000RPM, the red curves are at 5,000RPM and the blue curve at 15,000RPM. Results for 2 throat gaps, see Fig. 7 (i.e., Throat #1 and Throat #2) are shown, where Throat #2 is larger than Throat #1. Throat #1 data are represented with dotted lines and solid lines for Throat #2. The efficiency of capture increase with the shaft speed (black-red-blue). After 2.5 rotations, the volume starts to fill up to 100% output to input. These numbers approach 100% since the flow is incompressible and the volume is retaining more fluid at a larger rate than the outflow. As mentioned earlier, it is not the desire to fill up the volume, but to have continuous volume of water in the shaded zone and air mostly
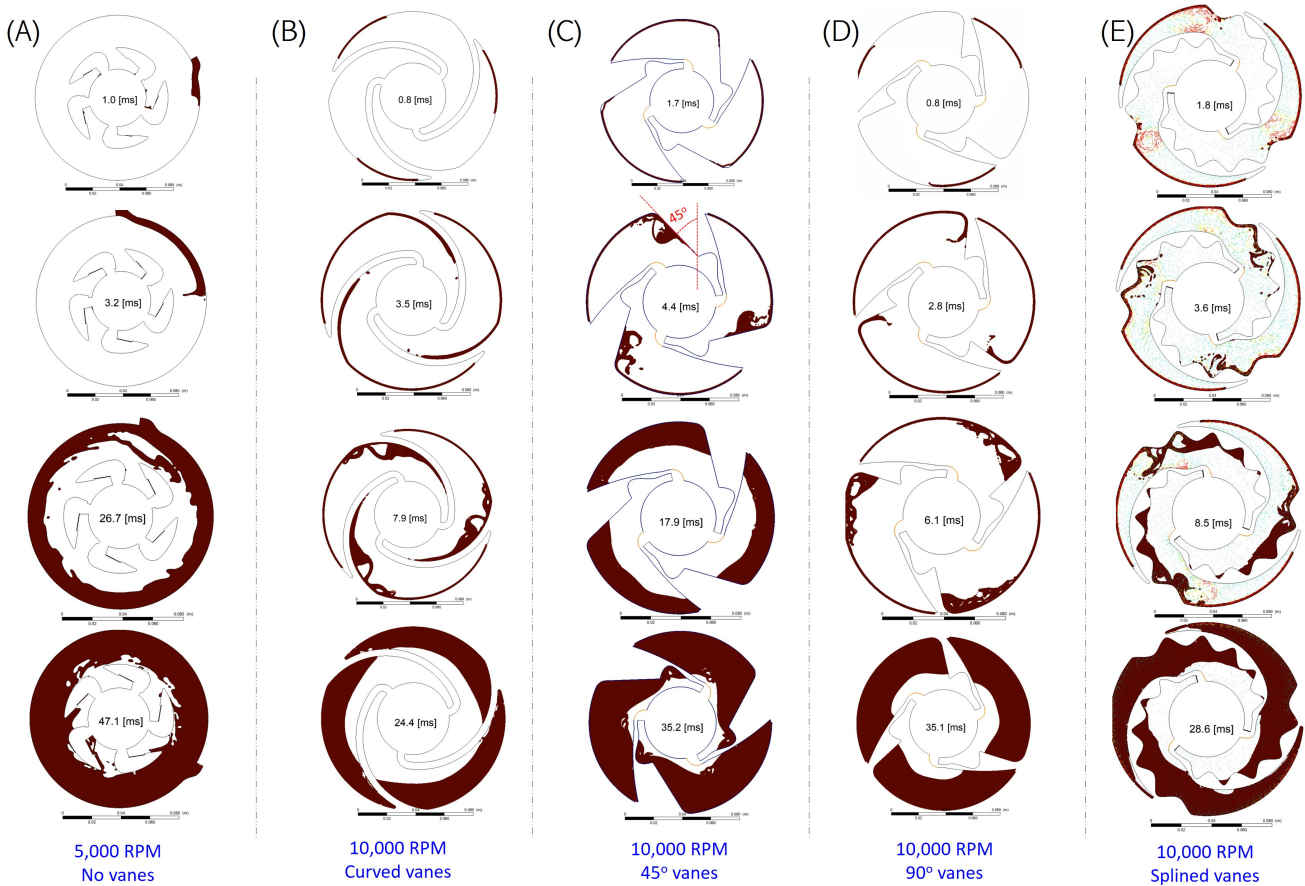
Figure 10: Behaviour of different blade profiles
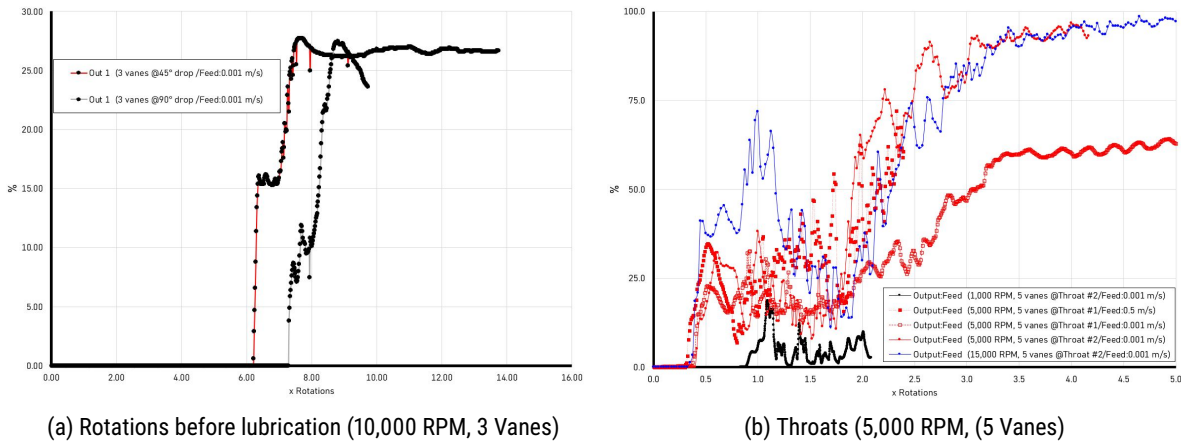
(a) Rotations before lubrication (10,000 RPM, 3 Vanes)

(b) Throats (5,000 RPM, (5 Vanes)

Figure 11: Outflow:Inflow ratio against number of rotations

outside of the that shaded zone as shown in the first top rows (Fig. 12). A design that results in having mostly air outside that shaded zone would mean little chance of backflow into stage 1. This figure therefore shows a better (than Fig. 10) design in terms of time to get initial lubrication to the bearing scoops, which is not observed in the other scoops in the first few rotations. There was however also a challenge of recirculation at the "throat" sections before the outlets. Opening the throat up seem to create lesser resistance above the bearing scoop but did not have significant difference on the output.

170
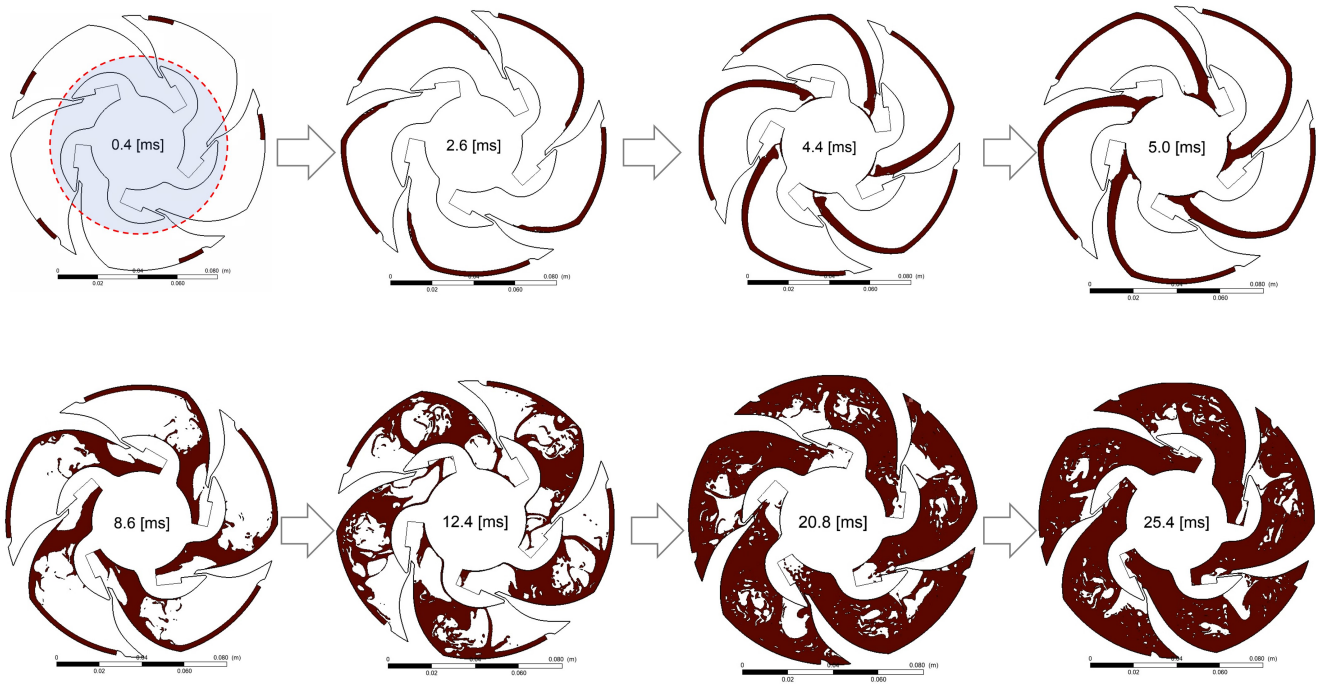
Figure 12: Staged vane

6   CONCLUSION

In this work, we proposed the use of a staging technique to improve the overall capture efficiency of a novel staged-scoops. Whereas, the first stage captures a jet of oil, in a set of inverted scoops, which is directed into a stage where the lubricant is made to flow against centrifugal and gravitational forces. The lubricant flows from a large diameter into a small diameter (bearing) shaft, with 5mm wide outlets. The experiment shows that using a high volume flow rate with minimal amount of splashing is achievable with inverted scoops. A series of conceptual design of the vanes, in stage 3, show that lubrication would happen even before the first revolution of the shaft, but a build-up of fluid in the throat region creates outflow resistance (recirculation) with a possibility for backflow into stage 1, thus limiting the overall capture efficiency of the scoop. Further work in optimising the throats to improve bearing lubrication or oil availability at the bearings is recommended.

ACKNOWLEDGEMENTS

REFERENCES

Adeniyi, A. A., H. Morvan, and K. Simmons (2017). "A computational fluid dynamics simulation of oil–air flow between the cage and inner race of an aero-engine bearing". *Journal of Engineering for Gas Turbines and Power* 139(1), page 012506.

Adeniyi, A. A., H. P. Morvan, and K. A. Simmons (2015). "A multiphase computational study of oil-air flow within the bearing sector of aeroengines". In: *Turbo expo: power for land, sea, and air.* Volume 56734. American Society of Mechanical Engineers, V05CT15A024.

Chandra, B., K. Simmons, S. Pickering, and M. Tittel (2010). "Factors affecting oil removal from an aeroengine bearing chamber". In: *Turbo Expo: Power for Land, Sea, and Air*. Volume 43963, pages 219–228.

Dai, Y., X. Chen, D. Yang, L. Xu, and X. Zhu (2022). "Performance of a New Aeronautic Oil-Guiding Splash Lubrication System". *Lubricants* 10(6), page 130.

Dhinesh, S., P. S. Arun, K. K. Senthil, and A. Megalingam (2021). "Study on flexural and tensile behavior of PLA, ABS and PLA-ABS materials". *Materials Today: Proceedings* 45, pages 1175–1180.

Eastwick, C., K. Simmons, Y. Wang, and S. Hibberd (2006). "Study of aero-engine oil-air separators". *Proceedings of the Institution of Mechanical Engineers, Part A: Journal of Power and Energy* 220(7), pages 707–717.

ExxonMobil (n.d.). *Mobil Jet Oil II*. `https://www.exxonmobil.com/en/aviation/products-and-services/products/mobil-jet-oil-ii`. Accessed: 2024-05-19.

Gao, W., D. Nelias, K. Li, Z. Liu, and Y. Lyu (2019). "A multiphase computational study of oil distribution inside roller bearings with under-race lubrication". *Tribology International* 140, page 105862.

Glahn, A. and S. Wittig (1996). "Two-phase air/oil flow in aero engine bearing chambers: characterization of oil film flows".

Jiang, L., Z. Liu, Y. Lyu, and J. Qin (2021). "Numerical simulation on the oil capture performance of the oil scoop in the under-race lubrication system". *Proceedings of the Institution of Mechanical Engineers, Part G: Journal of Aerospace Engineering* 235(15), pages 2258–2273.

Jiang, L., Y. Lyu, Y. Li, Y. Liu, Y. Hou, and Z. Liu (2023). "Numerical and Experimental Investigations to Assess the Impact of an Oil Jet Nozzle with Double Orifices on the Oil Capture Performance of a Radial Oil Scoop". *Aerospace* 10(12), page 1015.

Jingwen, Q., G. Hui, H. Jiang, W. Fuliang, M. Weiwei, and L. Yaguo (2021). "Novel design and simulation of curved blade oil scoop with high oil capture efficiency". *Chinese Journal of Aeronautics* 34(9), pages 94–103.

Kumar, N. and R. Satapathy (2023). "Bearings in aerospace, application, distress, and life: a review". *Journal of Failure Analysis and Prevention* 23(3), pages 915–947.

Lee, J., A. Prabhakar, and K. Johnson (2020). "Numerical investigations into the oil capture efficiency of a curve-bladed scoop system". In: *Turbo Expo: Power for Land, Sea, and Air*. Volume 84089. American Society of Mechanical Engineers, V02CT35A032.

Lopes, A. v. B., U. Thiele, and A. L. Hazel (2018). "On the multiple solutions of coating and rimming flows on rotating cylinders". *Journal of Fluid Mechanics* 835, pages 540–574.

Paleo Cageao, P., K. Simmons, A. Prabhakar, and B. Chandra (2019). "Assessment of the oil scoop capture efficiency in high speed rotors". *Journal of Engineering for Gas Turbines and Power* 141(1), page 012401.

Ren, G., Y. Li, H. Zhao, Y. Yan, W. Xu, and D. Sun (2023). "Research on Oil–Gas Two-Phase Flow Characteristics and Improvement of Aero-Engine Bearing Chamber". *Lubricants* 11(9), page 360.

Sadeghi, H., L. Diosady, and B. Blais (2022). "A computational fluid dynamics study on rimming flow in a rotating cylinder". *Physics of Fluids* 34(6).

Simmons, K. and B. Chandra (2014). "Experimental investigation into the performance of shallow aeroengine off-takes". In: *Turbo Expo: Power for Land, Sea, and Air*. Volume 45738. American Society of Mechanical Engineers, V05CT16A022.

Willenborg, K., S. Busam, H. Roßkamp, and S. Wittig (2002). "Experimental studies of the boundary conditions leading to oil fire in the bearing chamber and in the secondary air system of aeroengines". In: *Turbo Expo: Power for Land, Sea, and Air*. Volume 36088, pages 739–747.

Zhang, L., X. Zhang, and Z. Liu (2020). "An efficient numerical method for pressure loss investigation in an oil/air separator with metal foam in an aero-engine". *Energies* 13(2), page 346.

Zhong, Y., T. Li, S. Qu, H. Huang, and Z. Zhang (2023). "Failure Analysis of Over-Temperature of Aero-Engine Bearing". *Journal of Failure Analysis and Prevention* 23(5), pages 1869–1879.